Near-infrared fluorescent dyes for enhanced contrast in optical mammography: phantom experiments

B. Ebert
U. Sukowski
D. Grosenick
H. Wabnitz
Physikalisch-Technische Bundesanstalt,
Abbestrasse 2-12,
D-10587 Berlin, Germany

K. T. Moesta
Klinik für Chirurgie und Chirurgische Onkologie,
Robert-Roessle-Klinik,
Universitätsklinikum Charité,
Campus Berlin-Buch,
Medizinische Fakultät der Humboldt-Universität,
Lindenberger Weg 80,
D-13125 Berlin, Germany

K. Licha
A. Becker
W. Semmler
Institut für Diagnostikforschung GmbH
    an der Freien Universität Berlin,
Spandauer Damm 130,
D-14050 Berlin, Germany

P. M. Schlag
Klinik für Chirurgie und Chirurgische Onkologie,
Robert-Roessle-Klinik,
Universitätsklinikum Charité,
Campus Berlin-Buch,
Medizinische Fakultät der Humboldt-Universität,
Lindenberger Weg 80,
D-13125 Berlin, Germany

H. Rinneberg
Physikalisch-Technische Bundesanstalt,
Abbestrasse 2-12,
D-10587 Berlin, Germany

Abstract. Optical mammography with near-infrared (NIR) light using time-domain, frequency-domain, or continuous-wave techniques is a novel imaging modality to locate human breast tumors. By investigating excised specimens of normal and diseased mamma tissue we were able to demonstrate that differences in their scattering properties are a poor predictive parameter for normal and diseased mamma tissue. This paper describes the application of a NIR dye to improve the differentiation between breast tumors and normal tissue in a rat model. The NIR dye furnished a high tumor-to-tissue contrast ratio (6:1) in fluorescence images. Furthermore, this dye was used to develop liquid scattering phantoms with absorbing and fluorescent inhomogeneities. Using frequency-domain and time-domain instrumentation these inhomogeneities were localized at sufficient contrast by their increased absorption and fluorescence. Contrast between inhomogeneities and surrounding medium could be improved by combining fluorescence and transmittance images. © *2001 Society of Photo-Optical Instrumentation Engineers.* [DOI: 10.1117/1.1350561]

1 Introduction

In the last decades numerous methods for screening breast cancer have been applied, including x-ray mammography (for an overview see Ref. 1), magnetic resonance imaging,[2,3] positron emission tomography,[4] and ultrasound.[5] During the last few years a great deal of effort was expended to develop instrumental systems for transilluminating the breast and the brain with near-infrared (NIR) light,[6–11] taking advantage of the fact that NIR light is nonionizing and harmless at doses sufficient for medical diagnosis. A disadvantage of NIR transillumination imaging is the low spatial resolution that results from multiple scattering of photons when thick tissues are investigated.[12–14] The contrast in optical mammograms is based on different scattering and absorption properties of tumor and normal tissue. The contrast in optical transillumination images[8,15] based on scattering alone is not sufficient to discriminate the different types of tissues. On the other hand, increased vascularization and blood volume of tumors allow us to detect the lesions at adequate contrast based on absorption differences.[8,16–18] However, the tumors detected in these *in vivo* studies are rather large and exhibit a high degree of angiogenesis, therefore hemoglobin contrasts. In images relying on differences in absorption small tumors might be overlooked because of a low degree of angiogenesis and of superimposed areas due to large blood vessels, if these areas interfere geometrically with the target tissue. In this case a different mechanism to create contrast is needed.

Troy et al.[19] reported on reduced scattering and absorption coefficients, determined *ex vivo* by about 115 histologically classified specimens from 88 patients. The absorption coefficient was, however, underestimated due to blood drainage during excision. These measured absorption coefficients, therefore, do not reflect malignant *in vivo* conditions. Only for five patients was the reduced scattering coefficient determined for tumor and corresponding normal tissue of the same patient. However, direct comparison of the two types of tissue

---

Address all correspondence to B. Ebert. Tel: +49 30 3481 384; Fax: +49 30 3481 505; E-mail: bernd.ebert@ptb.de

for the same individual is crucial because of the large biological variability of normal breast tissue.

As a basis for the development of a contrast agent-based transillumination, for about 20 patients it was determined if there was a difference in the reduced scattering coefficients between normal and tumor tissue of the same patient. Since the alteration of tissue scattering properties by exogenous agents would require pharmacologically adjusted compounds, e.g., small air-filled particles with tumor-localizing properties (which are expected to be difficult to achieve) we focused on NIR dyes modifying tissue absorption and fluorescence. The use of a fluorescent contrast agent with high affinity to tumor tissue might be the method of choice[15,20,21] to overcome present limitations of optical transillumination imaging. A detailed theoretical description of the propagation of fluorescence photons in homogeneous media with a local inhomogeneity is given in Refs. 22 and 23. The use of fluorescent contrast agents with excellent enrichment was described in phantoms,[24] and subsequently applied in animal studies (dogs) for the detection of naturally occurring mammary disease[25,26] in reflection mode. In these studies photomultiplier-based and intensified charge coupled device (CCD)-based frequency-domain measurements were taken.

The aim of the present study was to investigate methods to improve the contrast of optical mammograms. One particular objective was to elucidate possible differences in the reduced scattering coefficient between tumor tissue and normal tissue of the human breast performing measurements *in vitro*. Second, we explored how contrast can be improved in transillumination images, using 5 cm thick liquid scattering phantoms with tissuelike optical properties and with a local inhomogeneity modeling a geometrically defined tumor area of enhanced absorption and fluorescence. To our knowledge, this is the first time such investigations have been performed using a time-domain mammograph. The particular NIR fluorescent dye used might be suitable as an optical contrast agent and was developed for the demarcation of mammary tumors by fluorescence.

2 Experiment

2.1 Examination of Tissue Specimens

Tumor tissues and normal tissue of the breast were investigated originating from a total of 20 patients who underwent primary surgical treatment for proven breast cancer. The specimens about 1 mm thick were placed between two glass plates (2 cm in diameter) immediately after excision and kept at 4 °C up to several hours before measurements were taken at 20 °C. The cylindrical sample holders were sealed by means of a 1 mm thick rubber O-ring to prevent desiccation of the sample. The scattering properties of tissue were derived from measurements of the diffuse transmittance and the diffuse reflectance for wavelengths between 600 and 800 nm using a two-integrating-sphere setup as described in Refs. 27 and 28. Every measurement lasted about 20 min and both samples were measured twice, the tumor sample always first. Within error limits (10%) both measurements gave the same results.

2.2 Fluorescent Optical Contrast Agent

As fluorescent dye we used the highly hydrophilic cyanine dye derivative 1,1′-bis-(4-sulfobutyl)indotricarbocyanine-

5,5′-dicarboxylic acid diglucamide monosodium salt (SIDAG).[29] Absorption spectra were measured using a Lambda-2 photometer (Perkin-Elmer GmbH, Überlingen, Germany). Fluorescence emission spectra of 2 μmol/L aqueous dye solutions were recorded in the front-face mode using a SPEX Fluorolog fluorometer (Instruments S.A. GmbH, Grasbrunn, Germany) consisting of single excitation and emission monochromators, a 350 W xenon lamp, and a photomultiplier (R928, Hamamatsu Deutschland GmbH, Herrsching, Germany).

2.3 *In vivo* Fluorescence Imaging

SIDAG was employed as a fluorescent marker for *in vivo* fluorescence imaging of mamma tumors in rats. The animal model is described in detail in Ref. 29. For fluorescence imaging the output pulses (pulse duration: 3 ns, wavelength: 740 nm, repetition rate: 50 Hz) of an optical parametric oscillator (OPO, GWU Lasertechnik, Erftstadt, Germany) pumped by the third harmonic (355 nm) of a Nd:YAG laser (GCR-230, Spectra Physics GmbH, Darmstadt, Germany) were used to excite the dye. The laser beam was expanded so that an area of about 250 mm in diameter was nearly homogeneously illuminated. Fluorescence images were recorded employing an intensified CCD camera (Spectroscopy Instruments GmbH, Grasbrunn, Germany) equipped with an optical band-pass filter to detect the wavelength range between 750 and 800 nm. The intensifier was opened by a 20 ns electrical pulse synchronized to the laser pulse and supplied by a high voltage generator (Avtech Electrosystems Ltd., Ottawa, Canada). In this way ambient light was suppressed in fluorescence images. For details of the experimental setup, see Ref. 30.

2.4 Phantom Experiments

Phantom experiments were performed on a liquid scattering phantom using a frequency-domain as well as a time-domain optical mammograph. For phantom experiments SIDAG was dissolved in a scattering solution consisting of a mixture of homogenized whole milk (volume concentration: 33%) and water containing 7% human serum albumin. The reduced scattering coefficient μ_s' of this liquid was approximately 14 cm^{-1} at λ=780 nm (estimated from time-resolved measurements). This value corresponds to the scattering properties of human breasts. Human serum albumin was added to improve the solubility of the dye and to simulate physiological conditions.

The phantom (phantom No. 1) used together with the frequency-domain optical mammograph consisted of a flat glass cuvette (x,y,z: 200, 200, and 50 mm), at the center of which (x=100 mm, z=25 mm) a rigid cylindrical tube (inner diameter 7 mm, length 200 mm) made of Teflon (wall thickness: 1 mm) was positioned as inhomogeneity. Teflon was chosen because of its scattering coefficient, which is close to that of breast tissue.

For experiments performed with the time-domain optical mammograph another glass cell (x, y, z: 200, 50, and 200 mm) was used (phantom No. 2). As inhomogeneity a cylindrical tube (inner diameter 7 mm, length 200 mm; wall thickness: $\approx$0.5 mm) made from dialysis tubing and closed at its lower end was placed vertically in the middle of the cell (x =100 mm, y=25 mm). The molecular weight cutoff of the

dialysis material (500 g/mol) was below the molecular weight of the dye (1089 g/mol), thus preventing the dye from leaking into the surrounding medium. To keep the flexible tube straight and aligned vertically, a small steel sphere (diameter 7 mm) was attached to the lower end of the tube.

Both cuvettes and tubes contained the solution described above as scattering medium. The NIR dye concentration in the bulk solution was chosen between 0.02 and 0.1 μmol/L, whereas the concentration in the tube was varied within certain limits taking data from animal models into account.[30]

The frequency-domain experiments were performed using the optical mammograph developed by Carl Zeiss, Oberkochen.[6,31] This mammograph was equipped with laser diodes emitting light at wavelengths of 690 and 810 nm modulated at a frequency of about 110 MHz. An avalanche photodiode served as detector. The apparatus was established at the Robert-Roessle-Klinik, Berlin-Buch, and used for examinations of patients.[32] The second part of the phantom studies was performed using a time-domain optical mammograph developed at the Physikalisch-Technische Bundesanstalt[8] and established at the Robert-Roessle-Klinik for investigation of patients. For the phantom experiments the mammograph was modified. The phantom was fixed in the compression unit and scanned in transmission mode, employing a transmitting fiber with 600 μm diameter and a receiving fiber bundle 4 mm in diameter. The glass plates used for compression of the breast were removed. The ps laser diodes of the mammograph were replaced by a mode-locked titanium–sapphire laser (Tsunami, Spectra Physics GmbH, Darmstadt, Germany) pumped by an argon ion laser (Innova Sabre, Coherent GmbH, Dieburg, Germany). The titanium–sapphire laser was operated at 750 nm and at a repetition rate of 80 MHz, and the width of the output pulses was about 2 ps. An average laser power of about 25 mW was applied to the phantom. Laser and fluorescence photons transmitted through the phantom were detected by a fast photomultiplier tube (PMT, H6279, Hamamatsu Deutschland GmbH, Herrsching, Germany). Distributions of times of flight were measured using the time-correlated single photon counting system (SPC 300, Becker&Hickl GmbH, Berlin, Germany) of the mammograph. The scanning step size was 2.5 mm and the collection time per pixel was 1 s, both for fluorescence and transmitted laser photons. Count rates for the transmitted laser light were adjusted to about 100 kHz by employing neutral density filters in front of the PMT corresponding to an attenuation factor of about 80. To detect fluorescence light, an optical band pass (760–800 nm) was used to block transmitted laser light. Furthermore, attenuation of the light by neutral density filters in front of the detector was reduced by a factor of about 10 to achieve similar count rates (80–100 kHz) as for transmitted laser light.

3 Results and Discussion

In Figure 1(a) the reduced scattering coefficient of tumor tissue and corresponding normal tissue is depicted in the wavelength range between 600 and 800 nm for a particular patient. As expected the reduced scattering coefficient decreases with increasing wavelength for both tumor and normal tissue in accordance with results obtained by Tromberg et al.[18] *in vivo* at six wavelengths between 670 and 960 nm. This wavelength dependence was similar for all specimens.
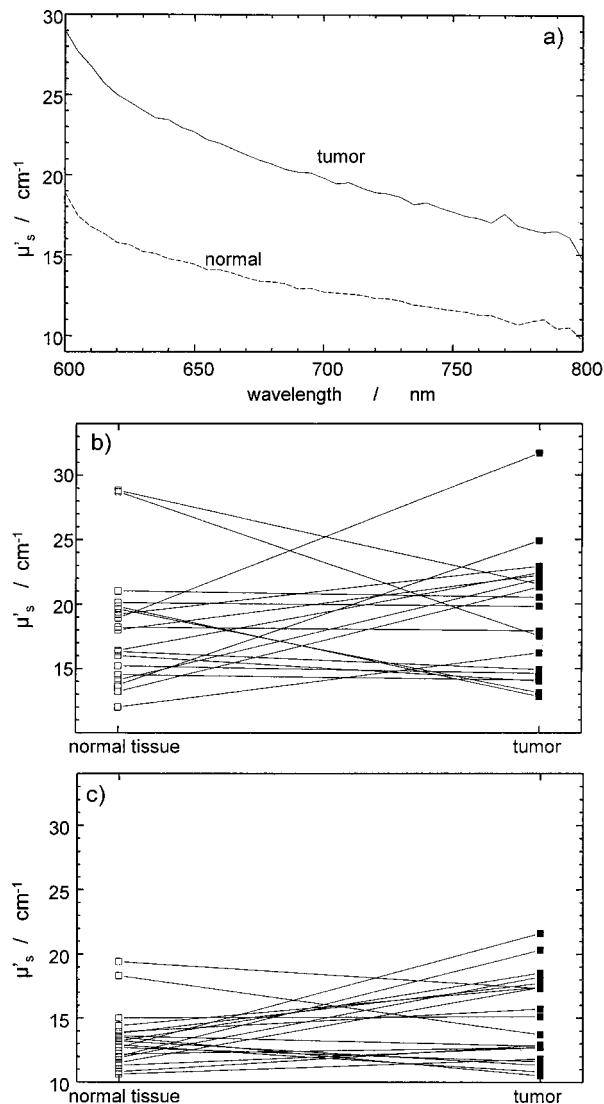
Fig. 1 Reduced scattering coefficient of tumor tissue and normal breast tissue of one selected patient versus wavelength (a). Reduced scattering coefficients of normal breast tissue and corresponding tumor tissue (connected by straight lines) of the same patient taken at λ=600 nm (b) and λ=700 nm (c). A total of 20 patients were investigated.

No general conclusions can be drawn from the ratios of the reduced scattering coefficients of tumor tissue and normal tissue *ex vivo*. This is evident from Figures 1(b) and 1(c) depicting the reduced scattering coefficients of tumor tissue and normal tissue obtained from 20 patients at λ=600 nm (b) and λ=700 nm (c). Obviously, the reduced scattering coefficients cannot be used to discriminate tumor and normal tissue. In Ref. 19 the same conclusion was reached. Absorption coefficients of tumor and normal tissue *in vivo* cannot be deduced from measurements *ex vivo*. In addition, it is known that detection of tumors in optical mammograms reflecting differences in absorption might be hampered by absorption of large blood vessels or of nonmalignant lesions. Therefore, we studied exogenous agents capable of adding biological specificity to optical imaging procedures, in particular optical mammography. For this purpose, we used the SIDAG tricarbocyanine
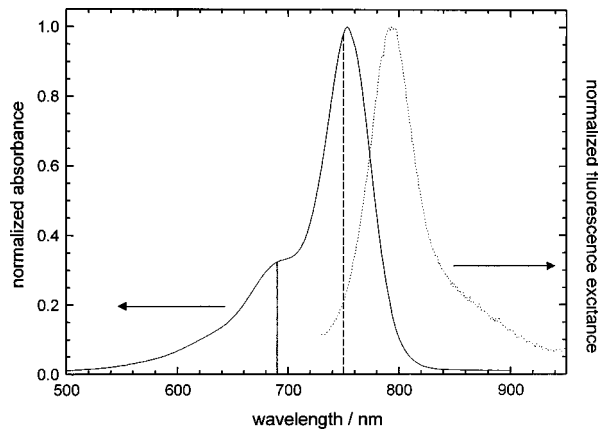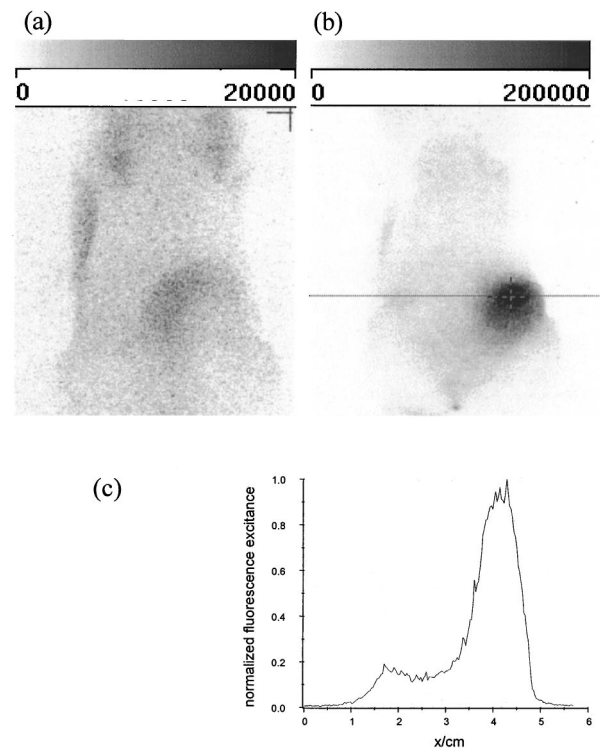
Fig. 2 Normalized absorption (solid line) and emission (dotted line) spectra of the dye SIDAG in bovine plasma (concentration 2 μmol/L). Vertical solid and dashed lines indicate the wavelengths used in the frequency-domain and the time-domain experiments, respectively.

Fig. 3 Fluorescence images of a tumor bearing rat (MTLn-3) at a dose of the dye SIDAG 2 μmol/kg body weight: (a) anterior view before i.v. administration and (b) anterior view 24 h after administration. Intensities are represented by gray scales corresponding to counts. It should be noted that the gray scales differ by a factor of 10. (c) Shows the fluorescence spectrum recorded along the dotted line of (b).

dye,[29,30] which exhibits a high extinction coefficient and a moderate fluorescence quantum yield.

In Figure 2 the normalized absorption and fluorescence emission spectra of the SIDAG fluorophor are shown. Due to the broad absorption spectrum peaked at 753 nm, the dye can be excited effectively between 670 and 750 nm. The wavelengths of the lasers used for frequency-domain and time-domain measurements are indicated by black solid and dashed lines, respectively. The fluorescence spectrum of SIDAG exhibits a maximum around 792 nm, which corresponds to a Stokes shift of about 40 nm. It follows that the major parts of the absorption and emission spectra cover a spectral range where scattering and absorption of tissue is low. This allows recording of fluorescence photons originating from thick tissue samples like the human breast.

Using this dye contrast enhancement between tumor and surrounding tissue was studied in a rat model with a tumor grown from the tumor cell line MTLn-3. As demonstrated by Riefke et al.,[20] this dye permitted demarcation of the tumor by fluorescence at the highest contrast about 24 h after intravenous injection. For illustration, fluorescence images of a tumor-bearing rat are shown in Figure 3. Figure 3(a) illustrates the fluorescence image prior to the application of the dye, Figure 3(b) the image taken 24 h after intravenous (i.v.) application of 2 μmol of SIDAG/kg of body weight. Figure 3(c) shows the normalized fluorescence intensity along the dotted line through the tumor [see Figure 3(b)] illustrating the high contrast between tumor and surrounding tissue. The fluorescence intensity of the remaining parts of the body was slightly higher than the autofluorescence intensity recorded initially. It follows that contributions from the SIDAG fluorescence were observed outside the tumor as well. The unspecific autofluorescence observed in rats can be caused by pheophorbides contained in the food. We have selected a specific diet to reduce this background fluorescence in animals.

We investigated whether at concentrations corresponding to *in vivo* data[29] this dye is suited to detect the inhomogeneity located 2.5 cm below the surface of phantom No. 1, simulating a compressed human breast of 5 cm thickness. Measurements were performed in transmission geometry using the frequency-domain mammograph and different concentrations of the dye inside the inhomogeneity of phantom No. 1. Source and detector optical fibers were moved in tandem in steps of 2 mm along a line crossing the tube. At each scan position amplitude modulation and phase shift were measured at the excitation wavelength of 690 nm. First, data were taken without any dye added to study the influence of the Teflon tube itself. Under these conditions the tube caused a phase shift of about 7° due to the higher reduced scattering coefficient of Teflon compared to the scattering solution. The tube was not visible in the modulation amplitude data, i.e., the absorption coefficient of the tube material was comparable to that of the scattering solution.

In Figure 4(a) normalized modulation amplitudes are shown recorded along the scan (x) direction. There was no dye added to the scattering medium surrounding the Teflon tube. The concentration of SIDAG inside the tube was varied between 0.2 and 2.0 μmol/L. Depending on the dye concentration, the modulation amplitude of the transmitted light was reduced from about 95% to 65% at the location of the tube. The reduction in modulation amplitude is caused by the increased absorption of the laser light inside the tube.

The normalized modulation amplitudes shown in Figure 4(b) correspond to a dye concentration of 0.1 μmol/L in the scattering medium surrounding the tube. Inside the tube, the concentration was varied between 0.1 and 0.8 μmol/L. Under these conditions, the absorption coefficient of the tube is no longer matched to that of the surrounding medium. When the
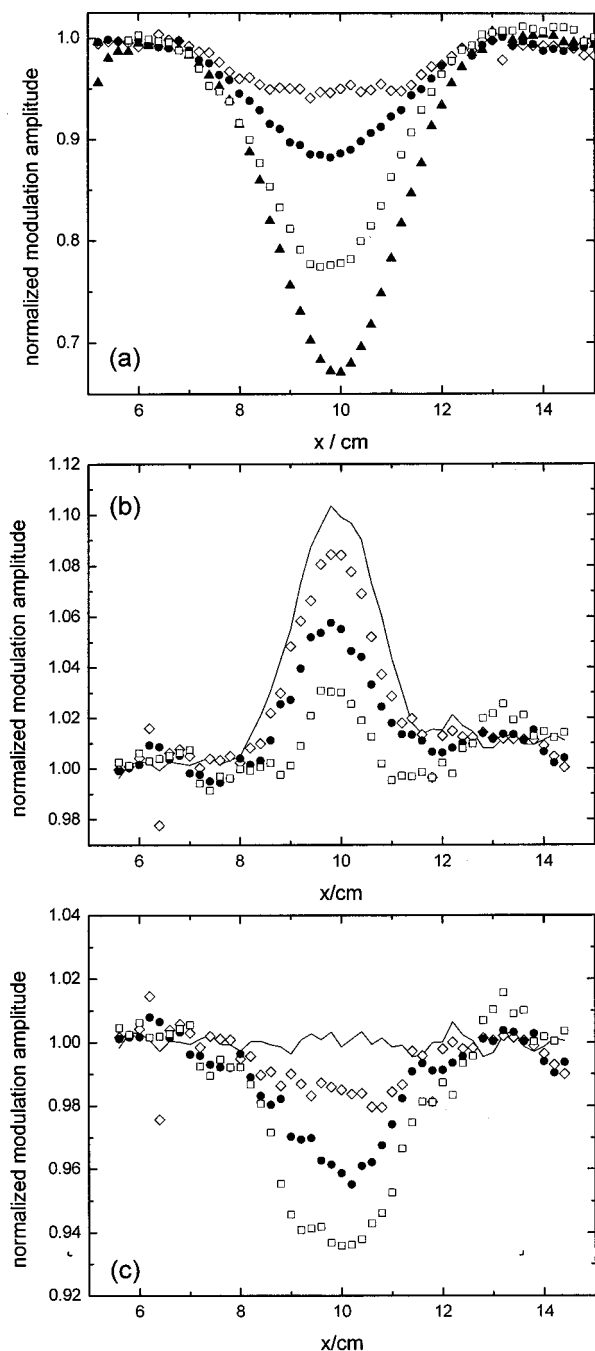
Fig. 4 Normalized modulation amplitudes along a line scan perpendicular to the Teflon tube at $x=10$ cm of phantom No. 1. The concentration of the dye within the tube was varied between 0.2 μmol/L (open diamonds), 0.5 μmol/L (closed circles), 1.0 μmol/L (open squares), and 2.0 μmol/L (closed triangles), no dye was added to the surrounding scattering solution (a). The dye concentration outside the tube was 0.1 μmol/L, the concentration within the tube was varied between 0.1 μmol/L (solid line), 0.2 μmol/L (open diamonds), 0.4 μmol/L (closed circles), and 0.8 μmol/L (open squares). (b) Taking the solid line of (b) as the baseline, (c) illustrates modulation amplitudes corrected for the influence of the wall of the tube.

dye concentrations of the scattering medium inside and outside the Teflon tube are the same (0.1 μmol/L) the smaller absorption by the Teflon should result in an increased modulation amplitude. This is visible in Figure 4(b) where the in-

crease in amplitude amounts to about 10% compared to the surrounding medium. Due to the mismatch in absorption coefficients between the tube and the scattering solutions this curve represents the baseline for investigations with other dye concentrations inside the tube. As expected, modulation amplitude decreases with respect to the baseline with increasing dye concentration inside the tube. Figure 4(c) shows the corresponding relative changes of the modulation amplitude with respect to the (smoothed) baseline. At the highest dye concentration used (0.8 μmol/L) the observed decrease in amplitude amounts to about 6%.

To minimize the influence of the tube material, we replaced the Teflon tube by a dialysis tube with a much thinner wall in phantom No. 2. This phantom was investigated using the time-domain mammograph. From distributions of time of flight of photons measured at the laser wavelength of 750 nm, photon counts in different time windows were calculated. Besides the total photon count N_{tot}, an early time window was analyzed extending from $t=0$ up to 1.73 ns. The width of the early time window was chosen such that at a reference position far from the inhomogeneity photon counts N_1 in this time window amounted to 10% of all photons N_{tot} detected at this position. When the scattering solution was the same inside and outside the tube it could not be detected by N_{tot} or N_1, independent of the dye concentration. Besides absorption of laser photons by the dye, we also investigated the fluorescence signal. To this end, the phantom was scanned a second time with a band pass filter in front of the detector to spectrally select the fluorescence signal. From measured distributions of times of flight of fluorescence photons, we determined total fluorescence photon counts $N_{tot,fl}$ and photon counts $N_{1,fl}$ in an early time window extending from $t=0$ up to 2.25 ns. Again, the early time window was chosen such that at the reference position photon counts $N_{1,fl}$ amounted to 10% of all fluorescence photons ($N_{tot,fl}$) detected at this position.

The results shown in Figure 5 were obtained at a dye concentration of 0.02 μmol/L in the surrounding medium and a tenfold higher dye concentration in the scattering solution contained in the tube. Figure 5(a) displays time-integrated intensity, i.e., N_{tot}, of transmitted laser photons normalized to the corresponding value at the reference position. At the position of the tube the number of transmitted photons detected is reduced by about 10% compared to the surrounding medium. A comparable reduction was obtained for early arriving photons. In Figure 5(b) the number of detected fluorescence photons $N_{1,fl}$ of the early time window is depicted, normalized to the corresponding value at the reference position. At the position of the tube $N_{1,fl}$ is higher by 10%, whereas the total intensity $N_{tot,fl}$ is larger by about 5% only. To improve contrast we have calculated the ratio of the fluorescence and transmittance signals depicted in Figures 5(b) and 5(a). Figure 5(c) shows the resulting image where contrast enhancement amounts to about 22%. In Figure 5(d) line scans are shown corresponding to the transmittance, fluorescence, and ratio images. The line scans were derived by averaging all eight scan lines of the images.

Our results may be compared to recent reports on NIR imaging of phantoms and tumors using protease activated fluorescent probes. Weissleder and co-workers[21,33] injected 250 pmol (5 μmol/L $\times$ 50 μL) of the dye Cy5.5 subcutane-
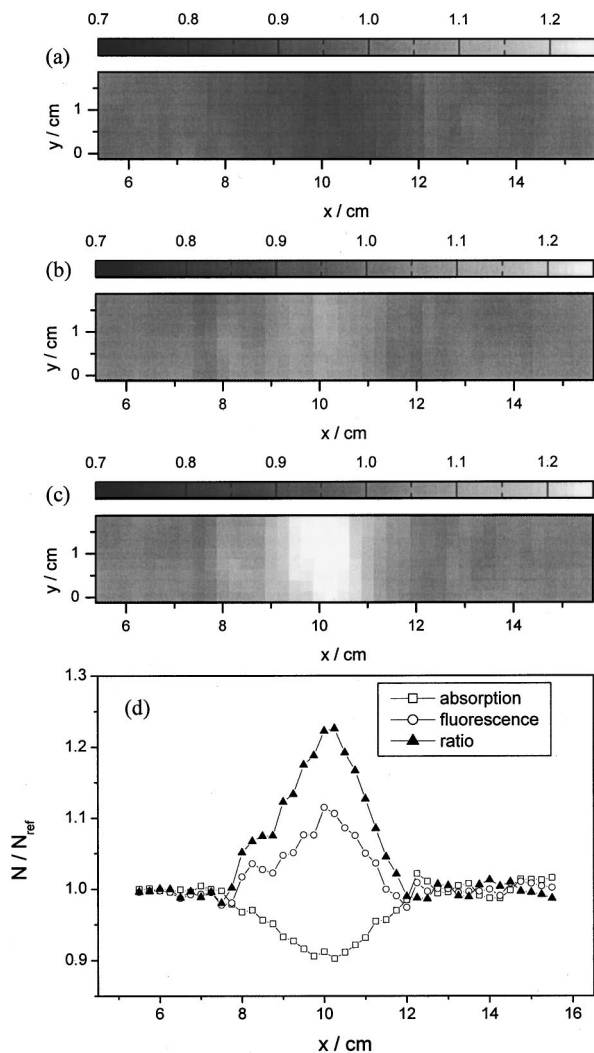
Fig. 5 Image of a cylindrical inhomogeneity 7 mm in diameter with a tenfold higher concentration of the fluorescence dye SIDAG compared to the surrounding medium (phantom No. 2). Normalized total photon counts N_{tot} at the laser wavelength (a). Normalized fluorescence photon counts $N_{1,fl}$ corresponding to the early time window (b). Ratio of normalized fluorescence phantom counts $N_{1,fl}$ and normalized total photon counts N_{tot} at the laser wavelength (c). Mean normalized photon counts and corresponding ratios derived from eight line scans along the x axis see [(a)–(c)], (d).

ously into the flank of nude mice. This amount could be detected through about 1 mm of skin at a signal/noise ratio=9.4 using a 10 s acquisition time. In our case (see Figure 5) the concentration of 1 μmol/L used corresponds to 385 pmol/cm tube length. The fluorescent object was detected against a fluorescing background at a contrast/noise ratio of about 5 through 5 cm of scattering solution at an acquisition time of 1 s per scan position. Although both experiments are not strictly comparable, the same amount of fluorescent dye was detected in each case.

We conclude this section by discussing the time required to record laser pulse fluorescence mammograms. It was shown in Ref. 8 that time-domain optical mammograms could be recorded within 3–5 min by sampling transmitted laser photons at each of 1000–2000 scan positions using 5 mW of

incident laser power and for breast thickness between 4 and 8 cm. It follows from our phantom experiments that fluorescence intensity for the dye concentrations investigated is weaker by at least a factor of 10–20 compared to excitation light. This reduced signal level could be partly compensated, e.g., by increasing data acquisition time or incident laser power, or by parallel data acquisition. Provided that similar dye concentrations and degrees of enrichment can be achieved *in vivo* as in our phantom experiments, recording of time-domain fluorescence mammograms may be feasible for compressed breasts of moderate thickness.

4 Conclusion

The *ex vivo* results presented in this paper illustrate that reduced scattering coefficients alone do not allow us to generally discriminate small (1 cm^3) breast tumors from normal breast tissue and from nonmalignant lesions of human breast with sufficient specificity. A promising way to improve the specificity of optical mammography is the application of contrast agents to modify the absorption and fluorescence properties of small tumors. It was shown that the SIDAG dye was enriched in a mammary tumor of a rat model up to a ratio of 6:1 and that no significant fluorescence originated from surrounding tissue. If this dye were approved for human studies it might favorably be used as a potential fluorescence tumor marker. Furthermore, we demonstrated that absorbing and fluorescent inhomogeneities containing this dye at concentrations as low as 0.2 μmol/L within a 5 cm thick, scattering, absorbing, and fluorescent phantom could be detected by recording time-resolved transmittance. Improved contrast was obtained by calculating the ratio of fluorescence and transmittance images, the latter taken at the wavelength of laser photons.

References

1. M. Säbel and H. Aichinger, ''Recent development in breast imaging,'' *Phys. Med. Biol.* **41**, 315–368 (1996).
2. R. J. Ross, J. S. Thompson, K. Kim, and R. A. Bailey, ''Nuclear magnetic resonance imaging and evaluation of human breast tissue: preliminary clinical trials,'' *Radiology* **143**, 195–205 (1982).
3. N. Dash, A. R. Lupetin, R. H. Daffner, Z. L. Deeb, R. J. Sefczek, and R. L. Schapiro, ''Magnetic resonance imaging in the diagnosis of breast tissue,'' *Am. J. Roentgenol.* **146**, 119–125 (1986).
4. A. Y. Rostom, J. Powe, A. Kandil, A. Ezzat, S. Bakheet, F. ElKhwsky, G. El-Hussainy, R. Sorbris, and O. Sjoklint, ''Positron emission tomography in breast cancer: a clinicopathological correlation of results,'' *Br. J. Radiol.* **72**, 1064–1068 (1999).
5. C. H. Jones, ''Methods of breast imaging,'' *Phys. Med. Biol.* **27**, 463–499 (1982).
6. H. Jess, H. Erdl, K. T. Moesta, and M. Kaschke, ''Light mammography with modulation technique,'' *Tech. Mess.* **66**, 220–233 (1996).
7. O. Klingenbeck, O. Schütz, and A. Oppelt, ''Mammographie mit Licht—Möglichkeiten und Grenzen,'' *Akt. Radiol.* **5**, 115–119 (1995).
8. D. Grosenick, H. Wabnitz, H. Rinneberg, K. T. Moesta, and P. M. Schlag, ''Development of a time-domain optical mammograph and first in vivo applications,'' *Appl. Opt.* **38**, 2927–2943 (1999).
9. J. H. Hoogenraad, M. B. v. d. Mark, S. B. Colak, G. W. 't Hooft, and E. S. v. d. Linden, ''First results from the Philips optical mammoscope,'' *Proc. SPIE* **3194**, 184–190 (1998).
10. F. E. W. Schmidt, E. F. Martin, E. M. C. Hillman, J. C. Hebden, and

D. T. Delpy, ''A 32-channel time-resolved instrument for medical optical tomography,'' *Rev. Sci. Instrum.* **71**, 256–265 (2000).

11. J. C. Hebden and D. T. Delpy, ''Diagnostic imaging with light,'' *Br. J. Radiol.* **70**, S206–S214 (1997).

12. H. Wabnitz and H. Rinneberg, ''Imaging in turbid media by photon density waves: spatial resolution and scattering relations,'' *Appl. Opt.* **36**, 64–74 (1997).

13. D. Grosenick, H. Wabnitz, and H. Rinneberg, ''Contrast and spatial resolution of time resolved transillumination scaling images,'' *Proc. SPIE* **2626**, 205–217 (1995).

14. D. Grosenick, H. Wabnitz, and H. Rinneberg, ''Time-resolved imaging of solid phantoms for optical mammography,'' *Appl. Opt.* **36**, 221–231 (1997).

15. L. Götz, S. H. Heywang-Köbrunner, O. Schütz, and H. Siebold, ''Optische Mammographie an präoperativen Patientinnen,'' *Akt. Radiol.* **8**, 31–33 (1998).

16. T. O. McBride, B. Pogue, E. D. Gerety, S. B. Poplak, U. L. Osterberg, and K. D. Paulsen, ''Spectroscopic diffuse optical tomography for the quantitative assessment of hemoglobin and oxygen saturation in breast tissue,'' *Appl. Opt.* **38**, 5480–5490 (1999).

17. S. B. Colak, M. B. van der Mark, G. W. Hooft, E. S. van der Linden, and F. A. Kuijpers, ''Clinical optical tomography and NIR spectroscopy for breast cancer detection,'' *IEEE J. Sel. Top. Quantum Electron.* **5**(4), 1143–1158 (1999).

18. B. J. Tromberg, N. Sha, R. Lanning, A. Cerussi, J. Espinoza, T. Phain, L. Svaasand, and J. Butler, ''Non-invasive in vivo characterization of breast tumors using photon migration spectroscopy,'' *Neoplasia* **2**, 26–40 (2000).

19. T. L. Troy, D. L. Page, and M. Sevick-Muraca, ''Optical properties of normal and diseased breast tissues: Prognosis for optical mammography,'' *J. Biomed. Opt.* **1**, 342–355 (1996).

20. B. Riefke, K. Licha, and W. Semmler, ''Kontrastmittel für die optische Mammographie,'' *Radiologe* **37**, 749–755 (1997).

21. R. Weissleder, C.-H. Tung, U. Mahmood, and A. Bogdanov, Jr., ''In vivo imaging of tumors with protease-activated near-infrared fluorescent probes,'' *Nat. Biotechnol.* **17**, 375–378 (1999).

22. X. D. Li, M. A. O'Leary, D. A. Boas, B. Chance, and A. G. Yodh, ''Fluorescent diffuse photon density waves in homogeneous and heterogeneous turbid media: analytic solutions and applications,'' *Appl. Opt.* **35**, 3746–3758 (1996).

23. D. Nolte, ''Erkennung und Abbildung pathologischer Gewebeveränderungen mittels laserinduzierter Fluoreszenz in vivo,'' PhD thesis, Freie Universität Berlin, Germany (1998).

24. E. M. Sevick-Muraca, G. Lopez, J. S. Reynolds, T. L. Troy, and C. L. Hutchinson, ''Fluorescence and absorption contrast mechanisms for biomedical optical imaging using frequency-domain techniques,'' *Photochem. Photobiol.* **66**, 55–64 (1997).

25. J. S. Reynolds, T. L. Troy, R. H. Mayer, A. B. Thompson, D. J. Waters, K. K. Cornell, P. W. Snyder, and E. M. Sevick-Muraca, ''Imaging of spontaneous canine mammary tumors using fluorescent contrast agents,'' *Photochem. Photobiol.* **70**, 87–94 (1999).

26. M. Gurfinkel et al., ''Pharmacokinetics of ICG and HPPH-car for the detection of normal and tumor tissue using fluorescence, near-infrared reflectance imaging: a case study,'' *Photochem. Photobiol.* **72**, 94–102 (2000).

27. U. Sukowski, B. Ebert, D. Nolte, and H. Rinneberg, ''Determination of transport scattering coefficients of phantoms and biological tissue in vivo for wavelengths between 600 nm and 800 nm,'' in *Proc. Technical Digest of EQEC'96, European Quantum Electronics Conference*, p. 157 (1996).

28. U. Sukowski, F. Schubert, D. Grosenick, and H. Rinneberg, ''Preparation of solid phantoms with defined scattering and absorption properties for optical tomography,'' *Phys. Med. Biol.* **43**, 1823–1844 (1996).

29. K. Licha, B. Riefke, V. Ntziachristos, A. Becker, B. Chance, and W. Semmler, ''Hydrophilic cyanine dyes as contrast agents for near-infrared tumor imaging: synthesis, photophysical properties and spectroscopic in vivo characterization,'' *Photochem. Photobiol.* **72**, 392–398 (2000).

30. B. Riefke, K. Licha, W. Semmler, D. Nolte, B. Ebert, and H. Rinneberg, ''In vivo characterization of cyanine dyes as contrast agents for near-infrared imaging,'' *Proc. SPIE* **2927**, 199–208 (1996).

31. S. Fantini, M. A. Franceschini, G. Gaida, E. Gratton, H. Jess, W. W. Matulin, K. T. Moesta, P. M. Schlag, and M. Kaschke, ''Frequency-domain optical mammography: edge effect corrections,'' *Med. Phys.* **23**, 149–157 (1996).

32. K. T. Moesta, S. Fantini, H. Jess, S. Totkas, M. A. Franceschini, M. Kaschke, and P. M. Schlag, ''Contrast features of breast cancer in frequency-domain laser scanning mammography,'' *J. Biomed. Opt.* **3**, 1–8 (1998).

33. U. Mahmood, C.-H. Tung, A. Bogdanov, Jr., and R. Weissleder, ''Near-infrared optical imaging of protease activity for tumor detection,'' *Radiology* **213**, 866–870 (1999).